Supplementary materials

S1. List of symbols and abbreviations

A	area
A_{H}	Hamaker constant
C	electrolyte concentration
D	diffusion coefficient
E	intensity of electric field
E_{G}	Gibbs elasticity of the membrane
e	elementary charge
j	electric current density
j_i	ion current density
H	height of the spherical cap made by the patch
h^{M}	thickness of the membrane
h^{S}	thickness of the seal
k_{B}	Boltzmann constant
L	wetted length of the capillary
L_{c}	length of the whole capillary
L_{D}	Debye length, $L_{\mathrm{D}}^2 = k_{\mathrm{B}}T\varepsilon / 2e^2C$
p	pressure
R	radius of curvature
R_{c}	radius of the capillary
R_i	Stokes radius of an ion
Res	electric resistance
Q	liquid delivery
T	temperature
t	time
$\boldsymbol{v}$	fluid velocity field
v_i	drift velocity
v_L	creep velocity, $v_L = \mathrm{d}L/\mathrm{d}t$
W	power

w power density

z coordinate normal to the glass surface

α cone top angle

Γ surface concentration of lipid in a monolayer

η viscosity

ε absolute dielectric permittivity

Π_{el} electrostatic contribution to the disjoining pressure

Π_{vdW} dispersion contribution to the disjoining pressure

ρ_e bulk charge density

ρ_e^G, ρ_e^M surface charge densities of the glass and the membrane

σ^M membrane tension

σ^G the surface tension of the glass

σ^{GM} the surface tension of the membrane-covered glass, $\sigma^{GM} = \sigma^G + \sigma^M - \sigma_{adh}$

σ_{adh} the adhesion energy ($\sigma_{adh} > 0$)

σ_{el} electrostatic contribution to the adhesion energy

σ_{vdW} dispersion contribution to the adhesion energy

ϕ electrostatic potential

ϕ^G, ϕ^M surface potentials of the glass and the outer wall of the membrane

ϕ_m minimal (midplane) potential of the film

ϕ_∞ surface potential of a free surface

subscripts:

$_{adh}$ adhered membrane

$_{cap}$ spherical cap

$_{c}$ capillary

superscripts:

^{G} glass

^{M} membrane

^{GM} glass with adhered membrane

S2. Electrostatics of the seal zone

To find the potential distribution $\phi^S(z)$ in the seal, we need to solve the Poisson-Boltzmann equation:

$$\varepsilon^S \nabla^2 \phi^S = -\sum e_i C_i \quad \text{with} \quad C_i = C_{i\infty} \exp(-e_i \phi^S / k_B T). \tag{A1}$$

The two surfaces (the glass $z = 0$ and the membrane $z = h^S$) are assumed to have fixed surface charge densities (ρ_e^G and ρ_e^M). This problem is long known[19]. Our main task now is, based on Derjaguin approach, to find for the case "constant charge" the difference $\Delta\phi = \phi^G - \phi^M$ as a function of h^S, in order to be able to use Eq (39) for the creep velocity, and to estimate the resistance of the seal using the obtained ion concentration profiles.

Briefly, Derjaguin integrated the Poisson-Boltzmann equation (A1) to obtain a solution for the potential in terms of the inverse function z vs. ϕ^S:

$$\frac{z}{L_D} = \pm \int_{\Phi_m}^{\Phi} \frac{d\Phi}{\Phi \sqrt{\Phi + \Phi^{-1} - \Phi_m - \Phi_m^{-1}}} . \tag{A2}$$

We use the following symbols for the electrostatic Boltzmann factors (used here as kind of dimensionless potentials):

$$\Phi = \exp\left(-e\phi^S / k_B T\right), \quad \Phi_m = \exp\left(-e\phi_m / k_B T\right),$$

$$\Phi^M = \exp\left(-e\phi^M / k_B T\right), \quad \Phi^G = \exp\left(-e\phi^G / k_B T\right); \tag{A3}$$

L_D is the Debye length; ϕ_m is the minimal potential (in a symmetric film, it lays in the middle of the film – Langmuir's "midplane potential" – but with asymmetric films such as the water film between glass and membrane this is not the case); z is distance from the plane of minimal potential.

The value of ϕ_m (or Φ_m) plays a central role in the electrostatic model of the film. This potential is a decaying function of h^S. According to Derjaguin's result Eq (A2), the distances h^{Mm} from the plane of minimal potential to the membrane and h^{Gm} from the plane of minimal potential to the glass surface are given by:

$$h^{Mm} = L_D \int_{\Phi_m}^{\Phi^M} \frac{d\Phi}{\Phi \sqrt{\Phi + \Phi^{-1} - \Phi_m - \Phi_m^{-1}}}; \quad h^{Gm} = L_D \int_{\Phi_m}^{\Phi^G} \frac{d\Phi}{\Phi \sqrt{\Phi + \Phi^{-1} - \Phi_m - \Phi_m^{-1}}} . \tag{A4}$$

The total thickness of the seal is $h^{\mathrm{S}} = h^{\mathrm{Mm}} + h^{\mathrm{Gm}}$; the above integrals can be expressed in terms of the elliptic $\mathrm{F_E}$ integrals; this yields the following equation for h^{S}:

$$\frac{h^{\mathrm{S}}}{L_{\mathrm{D}}} = -2\mathrm{i}\sqrt{\frac{\Phi_{\mathrm{m}}}{\Phi_{\mathrm{m}}^2 - 1}}\left[\mathrm{F_E}\left(\mathrm{i}\sqrt{\frac{\Phi^{\mathrm{M}} - \Phi_{\mathrm{m}}}{\Phi_{\mathrm{m}}}}, \frac{\Phi_{\mathrm{m}}}{\sqrt{\Phi_{\mathrm{m}}^2 - 1}} \right) + \mathrm{F_E}\left(\mathrm{i}\sqrt{\frac{\Phi^{\mathrm{S}} - \Phi_{\mathrm{m}}}{\Phi_{\mathrm{m}}}}, \frac{\Phi_{\mathrm{m}}}{\sqrt{\Phi_{\mathrm{m}}^2 - 1}} \right) \right]; \qquad \text{(A5)}$$

here $\mathrm{i} = \sqrt{-1}$. This equation determines implicitly the dependence $\phi_{\mathrm{m}}(h^{\mathrm{S}})$. If the film thinning is in constant potential regime, then $\Phi^{\mathrm{M}} = \Phi_{\infty}{}^{\mathrm{M}}$ and $\Phi^{\mathrm{G}} = \Phi_{\infty}{}^{\mathrm{G}}$ ($\Phi_{\infty}{}^{\mathrm{M}}$ and $\Phi_{\infty}{}^{\mathrm{G}}$ being the unperturbed potential of the free membrane and glass) and the relation (A5) can be directly used to calculate the inverse function $h^{\mathrm{S}}(\phi_{\mathrm{m}})$. However, in constant charge regime, Φ^{M} and Φ^{S} also depend on h^{S}. This dependence must be determined from the thin film analogs of the Gouy equation (surface electroneutrality). At the glass surface, the Gouy equation reads[19]:

$$\frac{eL_{\mathrm{D}}\rho_e^{\mathrm{G}}}{\varepsilon^{\mathrm{S}} k_{\mathrm{B}} T} = -\sqrt{\Phi^{\mathrm{G}} + \left(\Phi^{\mathrm{G}}\right)^{-1} - \Phi_{\mathrm{m}} - \Phi_{\mathrm{m}}^{-1}}\,. \qquad \text{(A6)}$$

At the outer membrane wall, Gouy equation is complicated by the fact that there is non-zero field inside the membrane. The electroneutrality condition states that:

$$\rho_e^{\mathrm{MS}} = -\varepsilon^{\mathrm{S}} \frac{\mathrm{d}\phi^{\mathrm{S}}}{\mathrm{d}z} + \varepsilon^{\mathrm{M}} \frac{\mathrm{d}\phi^{\mathrm{membrane}}}{\mathrm{d}z}\,. \qquad \text{(A7)}$$

Using the first integral of Poisson-Boltzmann equation[19],

$$\frac{\mathrm{d}\phi^{\mathrm{S}}}{\mathrm{d}z} = \frac{k_{\mathrm{B}} T}{eL_{\mathrm{D}}} \sqrt{\Phi^{\mathrm{M}} + \left(\Phi^{\mathrm{M}}\right)^{-1} - \Phi_{\mathrm{m}} - \Phi_{\mathrm{m}}^{-1}} > 0\,, \qquad \text{(A8)}$$

and the fact that the field in the membrane is linear,

$$\frac{\mathrm{d}\phi^{\mathrm{membrane}}}{\mathrm{d}z} = \frac{\phi^{\mathrm{M}} - \phi^{\mathrm{C}}}{h^{\mathrm{M}}} < 0\,, \qquad \text{(A9)}$$

we obtain the following electroneutrality condition (generalizing the Gouy equation):

$$\frac{eL_{\mathrm{D}}\rho_e^{\mathrm{M}}}{\varepsilon^{\mathrm{S}} k_{\mathrm{B}} T} = -\sqrt{\Phi^{\mathrm{M}} + \left(\Phi^{\mathrm{M}}\right)^{-1} - \Phi_{\mathrm{m}} - \Phi_{\mathrm{m}}^{-1}} + \frac{\varepsilon^{\mathrm{M}} eL_{\mathrm{D}}}{\varepsilon^{\mathrm{S}} k_{\mathrm{B}} T} \frac{\phi^{\mathrm{M}} - \phi^{\mathrm{C}}}{h^{\mathrm{M}}}\,; \qquad \text{(A10)}$$

here ϕ^{C} is the surface potential at the membrane-cell boundary (the inner monolayer of the membrane). However, the term proportional to ρ_e^{M} is of the order of 2÷20, while the correction term for the field in the membrane is 0.02÷0.2, therefore, we can neglect the correction term to obtain

$$\frac{eL_{\mathrm{D}}\rho_e^{\mathrm{M}}}{\varepsilon^{\mathrm{S}}k_{\mathrm{B}}T}=-\sqrt{\Phi^{\mathrm{M}}+\left(\Phi^{\mathrm{M}}\right)^{-1}-\Phi_{\mathrm{m}}-\Phi_{\mathrm{m}}^{-1}}\,. \tag{A11}$$

Physically, this approximation means that the charge located at the inner wall of the membrane does not affect significantly the field distribution in the seal. This approximation simplifies the multilayer problem to Derjaguin's asymmetric thin film.

We can compare Eqs (A6) and (A11) with the normal Gouy equations for a free glass or membrane surface, obtained using the thick film limit, where $\phi_{\mathrm{m}} = 0$ ($\Phi^{\mathrm{M}} = 1$):

$$\frac{eL_{\mathrm{D}}\rho_e^{\mathrm{G}}}{\varepsilon^{\mathrm{S}}k_{\mathrm{B}}T}=-\sqrt{\Phi_\infty^{\mathrm{G}}+\left(\Phi_\infty^{\mathrm{G}}\right)^{-1}-2}\,;\qquad \frac{eL_{\mathrm{D}}\rho_e^{\mathrm{M}}}{\varepsilon^{\mathrm{S}}k_{\mathrm{B}}T}=-\sqrt{\Phi_\infty^{\mathrm{M}}+\left(\Phi_\infty^{\mathrm{M}}\right)^{-1}-2}\,. \tag{A12}$$

Using Eqs (A12), we can write Eqs (A6) and (A11) in their somewhat more operative forms in which surface charge densities ρ_e^{G} and ρ_e^{M} are eliminated:

$$\Phi_\infty^{\mathrm{G}}+\left(\Phi_\infty^{\mathrm{G}}\right)^{-1}-2=\Phi^{\mathrm{G}}+\left(\Phi^{\mathrm{G}}\right)^{-1}-\Phi_{\mathrm{m}}-\Phi_{\mathrm{m}}^{-1}; \tag{A13}$$

$$\Phi_\infty^{\mathrm{M}}+\left(\Phi_\infty^{\mathrm{M}}\right)^{-1}-2=\Phi^{\mathrm{M}}+\left(\Phi^{\mathrm{M}}\right)^{-1}-\Phi_{\mathrm{m}}-\Phi_{\mathrm{m}}^{-1}. \tag{A14}$$

Eqs (A13), (A14) and (A5) are a system of 3 equations for the 3 potentials, ϕ_{m}, ϕ^{G} and ϕ^{M}, as functions of h^{S}. They are exact within the limits of validity of Poisson-Boltzmann equation, the constant charge assumption and the assumption of a negligible contribution of the charge of the inner wall of the membrane. A parametrical solution $h^{\mathrm{S}}(\phi_{\mathrm{m}})$, $\phi^{\mathrm{S}}(\phi_{\mathrm{m}})$ and $\phi^{\mathrm{G}}(\phi_{\mathrm{m}})$ is easily obtained and it is shown in Figure 2.

This solution also determines the repulsive electrostatic force between the glass and the membrane. Langmuir's classical expression for the disjoining pressure is still valid for asymmetric film[19]:

$$\Pi_{\mathrm{el}}=k_{\mathrm{B}}TC\left(\Phi_{\mathrm{m}}+\Phi_{\mathrm{m}}^{-1}-2\right). \tag{A15}$$

Together with $h^{\mathrm{S}}(\phi_{\mathrm{m}})$, this equation determines the dependence of the electrostatic contribution to the adhesion energy on h^{S}. We will only analyze the limit of Π_{el} at $h^{\mathrm{S}} >> L_{\mathrm{D}}$. Using the asymptote

$$\int_{\Phi_{\mathrm{m}}}^{\Phi}\frac{1}{\Phi\sqrt{\Phi+\Phi^{-1}-\Phi_{\mathrm{m}}-\Phi_{\mathrm{m}}^{-1}}}\mathrm{d}\Phi\xrightarrow{\Phi_{\mathrm{m}}\to 1}\ln\frac{4\left(\sqrt{\Phi}-1\right)}{\left(\sqrt{\Phi}+1\right)\left(\sqrt{\Phi_{\mathrm{m}}}-1\right)}, \tag{A16}$$

we can write instead of Eq (A5)

$$\frac{h^{\mathrm{S}}}{L_{\mathrm{D}}} \xrightarrow{\Phi_{\mathrm{m}}\to 1} \ln \frac{16\left(\sqrt{\Phi^{\mathrm{G}}}-1\right)\left(\sqrt{\Phi^{\mathrm{M}}}-1\right)}{\left(\sqrt{\Phi^{\mathrm{G}}}+1\right)\left(\sqrt{\Phi^{\mathrm{M}}}+1\right)\left(\sqrt{\Phi_{\mathrm{m}}}-1\right)^{2}}. \tag{A17}$$

This equation is easily solved for Φ_{m}. The result is substituted into Eq (A15) to obtain Eq (4). The electrostatic energy (5) is then obtained from the result for Π_{el} using the relation $\Pi_{\mathrm{el}} = -\mathrm{d}\sigma_{\mathrm{el}}/\mathrm{d}h^{\mathrm{S}}$.

All of the above are well-known "classic" formulae. A new point with our problem is that our liquid film is extremely thin, which complicates the problem. Let us obtain some simple analytical results for the case where it is so thin that $h^{\mathrm{S}} < L_{\mathrm{D}}$. We use, first, the approximation $\Phi^{\mathrm{G}} >> 1/\Phi^{\mathrm{G}}$ and $\Phi^{\mathrm{M}} >> 1/\Phi^{\mathrm{M}}$, which are fulfilled even for thicker films. This simplifies our Gouy equations and leads to explicit expressions for Φ^{S} and Φ^{M}:

$$\Phi^{\mathrm{G}} = \Phi_{\mathrm{m}} + \Phi_{\infty}^{\mathrm{G}} + \left(\Phi_{\infty}^{\mathrm{G}}\right)^{-1} - 2; \qquad \Phi^{\mathrm{M}} = \Phi_{\mathrm{m}} + \Phi_{\infty}^{\mathrm{M}} + \left(\Phi_{\infty}^{\mathrm{M}}\right)^{-1} - 2. \tag{A18}$$

Substituting these into Eq (A5) for Φ_{m} vs. h^{S} and using another approximation – $\Phi_{\mathrm{m}} \approx \Phi^{\mathrm{M}} \approx \Phi^{\mathrm{G}}$, valid for $h^{\mathrm{S}} << L_{\mathrm{D}}$ (cf. Figure 2) by taking the series expansion of the elliptic functions we obtain the following equation:

$$\frac{h^{\mathrm{S}}}{L_{\mathrm{D}}} = 2\sqrt{\frac{\Phi_{\infty}^{\mathrm{M}} - \Phi_{\mathrm{m}}}{\Phi_{\mathrm{m}}^{2} - 1}} + 2\sqrt{\frac{\Phi_{\infty}^{\mathrm{G}} - \Phi_{\mathrm{m}}}{\Phi_{\mathrm{m}}^{2} - 1}} \approx 2\sqrt{\frac{\Phi_{\infty}^{\mathrm{M}} - \Phi_{\mathrm{m}}}{\Phi_{\mathrm{m}}^{2}}} + 2\sqrt{\frac{\Phi_{\infty}^{\mathrm{G}} - \Phi_{\mathrm{m}}}{\Phi_{\mathrm{m}}^{2}}}. \tag{A19}$$

This equation is easily solved for Φ_{m}; the result is then substituted into Eqs (A18) and the later are further simplified to yield the sought difference $\Delta\phi = \phi^{\mathrm{G}} - \phi^{\mathrm{M}}$ as a function of h^{S}:

$$\Delta\phi = \frac{k_{\mathrm{B}}T}{2e}\left[\left(\Phi_{\infty}^{\mathrm{M}}\right)^{-1/2} - \left(\Phi_{\infty}^{\mathrm{G}}\right)^{-1/2}\right]\left[\left(\Phi_{\infty}^{\mathrm{M}}\Phi_{\infty}^{\mathrm{G}}\right)^{1/2} + 1\right]\frac{h^{\mathrm{S}}}{L_{\mathrm{D}}}. \tag{A20}$$

This equation is equivalent to Eq (7).

S3. Effect of surface conductivity on seal resistivity

When the surface potential is high and the seal film has a thickness comparable to L_D, the surface conductivity starts to play a role in the seal resistance. The increased concentration of counterions in the surface vicinity, $C_i = C_{i\infty}\exp(-e_i\phi/k_BT)$, increases the electric current under the action of E:

$$J = 2\pi R_c \sum \Lambda_i \int_0^{h^S} C_{i\infty} \exp(-e_i\phi / k_B T)\mathrm{d}zE = 2\pi R_c h^S \sum \Lambda_i C_{i\infty} \left(1 + con_i^S\right)E \,, \tag{A21}$$

where Λ_i is the ionic conductivity of the i-th ion and con_i^S is the contribution for the surface conductivity of the i-th ion to J:

$$con_i^S = \frac{1}{h^S}\int_0^{h^S} \left(\exp(-e_i\phi / k_B T) - 1\right)\mathrm{d}z \,. \tag{A22}$$

Assuming for simplicity that both ions have the same mobilities, we find

$$J = 2\pi R_c \sum \Lambda_i \int_0^{h^S} C_{i\infty} \exp(-e_i\phi / k_B T)\mathrm{d}zE = 4\pi R_c h^S \Lambda_i C \left(1 + con^S\right)E \,, \tag{A23}$$

where $$con^S = \frac{1}{2h^S}\int_0^{h^S} \left(\Phi + 1/\Phi - 2\right)\mathrm{d}z \,. \tag{A24}$$

If $h^S > L_D$, the conductivity can be divided in two contributions from the two surfaces:

$$con^S \approx con^G + con^M \,. \tag{A25}$$

The contribution con^G refers to the double layer of the glass surface only, i.e.,

$$con^G = \frac{1}{2h^S}\int_G \left(\Phi + 1/\Phi - 2\right)\mathrm{d}z = \frac{1}{2h^S}\int_1^{\Phi^G} \frac{\Phi + 1/\Phi - 2}{\mathrm{d}\Phi/\mathrm{d}z}\mathrm{d}\Phi \,, \tag{A26}$$

where the integration is performed as if the glass surface is free. Using the first integral of Poisson-Boltzmann equation[19,16], $(\mathrm{d}\Phi/\mathrm{d}z)^2 = \Phi^2(\Phi + 1/\Phi - 2)/L_D^2$, we can take the integral analytically:

$$con^G = \frac{L_D}{h^S}\left[\left(\Phi^G\right)^{1/2} + \left(\Phi^G\right)^{-1/2} - 2\right]. \tag{A27}$$

Similarly, for the conductivity of the membrane surface, we obtain:

$$con^M = \frac{L_D}{h^S}\left[\left(\Phi^M\right)^{1/2} + \left(\Phi^M\right)^{-1/2} - 2\right]. \tag{A28}$$

Substituting these into Eq (A23), we obtain for the resistivity the expression (13).

S4. Ratio between van der Waals attractive energy and the energy of the repulsive interactions in equilibrium thin films

Consider a film in which an attractive dispersion interaction is acting together with certain repulsive force. We choose for simplicity a simple exponential dependence for the repulsion (which can refer to electrostatic repulsion, Eq (5), but other repulsive interactions also[12,29] follow approximately exponential dependences on h), and the simplest h^{-2} law for the attraction, i.e.,

$$\sigma_{\mathrm{adh}} = \frac{A_{\mathrm{H}}}{12\pi h^2} - A_{\mathrm{R}} \exp(-h / L_{\mathrm{R}}), \tag{A29}$$

where L_{R} is the characteristic length of the repulsive force (Debye length for electrostatics, hydration length for hydration repulsion etc.); A_{R} is a positive coefficient. The derivatives of σ_{adh} are:

$$\frac{\partial \sigma_{\mathrm{adh}}}{\partial h} = -\frac{A_{\mathrm{H}}}{6\pi h^3} + \frac{A_{\mathrm{R}}}{L_{\mathrm{R}}} \exp(-h / L_{\mathrm{R}}); \quad \frac{\partial^2 \sigma_{\mathrm{adh}}}{\partial h^2} = \frac{A_{\mathrm{H}}}{2\pi h^4} - \frac{A_{\mathrm{R}}}{L_{\mathrm{R}}^2} \exp(-h / L_{\mathrm{R}}). \tag{A30}$$

If A_{R} is small enough, then $\sigma_{\mathrm{adh}}(h)$ is a monotonically decreasing function. Above certain critical value of A_{R}, the adhesion energy σ_{adh} will possess a maximum and a minimum with respect to h. The critical value itself corresponds to saddle point of the function $\sigma_{\mathrm{adh}}(h)$ where both $\partial\sigma_{\mathrm{adh}}/\partial h$ and $\partial^2\sigma_{\mathrm{adh}}/\partial h^2$ are zero; from Eqs (A30) it follows that this saddle point is at:

$$h_{\mathrm{cr}} = 3L_{\mathrm{R}}; \quad A_{\mathrm{R,cr}} = \frac{\mathrm{e}^{-3} A_{\mathrm{H}}}{162\pi L_{\mathrm{R}}^2}. \tag{A31}$$

The maximum of σ_{adh}, which corresponds to the equilibrium state of the film, is always at $h_{\mathrm{eq}} > h_{\mathrm{cr}}$. This maximum is obtained from the extremum condition $\partial\sigma_{\mathrm{adh}}/\partial h = 0$, which yields:

$$\frac{A_{\mathrm{R}}}{L_{\mathrm{R}}} \exp(-h_{\mathrm{eq}} / L_{\mathrm{R}}) = \frac{A_{\mathrm{H}}}{6\pi h_{\mathrm{eq}}^3}. \tag{A32}$$

This is a transcendental equation for the equilibrium thickness h_{eq}; we do not need to solve it for our purposes. We substitute the exponent in Eq (A29) according to Eq (A32) to obtain the equilibrium adhesion energy:

$$\sigma_{\mathrm{adh,eq}} = \frac{A_{\mathrm{H}}}{12\pi h_{\mathrm{eq}}^2}\left(1 - \frac{2L_{\mathrm{R}}}{h_{\mathrm{eq}}}\right) = \left|\sigma_{\mathrm{vdW,eq}}\right|\left(1 - \frac{2L_{\mathrm{R}}}{h_{\mathrm{eq}}}\right); \tag{A33}$$

here, $-A_H/12\pi h_{eq}^2$ is obviously the van der Waals energy $\sigma_{vdW,eq}$ of the equilibrium film. From Eq (A33), we find that

$$\left|\frac{\sigma_{adh,eq}}{\sigma_{vdW,eq}}\right| = 1 - \frac{2L_R}{h_{eq}}. \tag{A34}$$

However, we found that $h_{eq} > 3L_R$, Eq (A31), so it is valid for the equilibrium film that

$$1 < \left|\frac{\sigma_{adh,min}}{\sigma_{vdW,min}}\right| < \frac{1}{3}. \tag{A35}$$

Similar estimations can be given for many other models for the surface forces in the film (electrostatic, steric or hydration repulsion, and more complex models of the van der Waals attraction). The final result is the same: whenever van der Waals force is the leading attractive term in the adhesion energy, then, irrespective of the nature of the repulsive force, $\sigma_{adh,eq}$ is of the order of or 2-5 times smaller than $|\sigma_{vdW,eq}|$. The estimation is inapplicable if the leading attractive term is not the van der Waals energy.

S5. Adhesion-driven creep in conical capillary

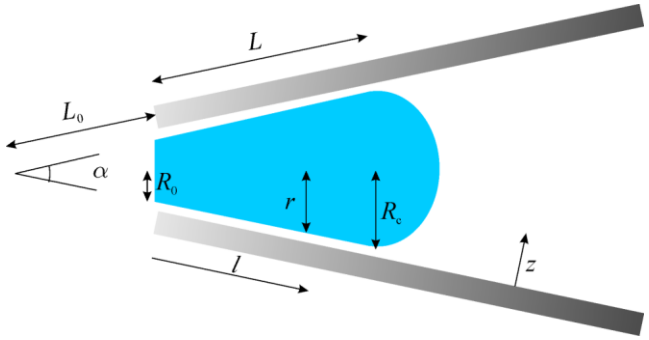

Figure S 1. Diagram of a conical capillary.

The geometrical characteristics of the pipette are defined in Figure S 1, together with their symbols. The following relations between these geometrical characteristics will be needed:

$$R_c = (L_0 + L)\sin(\alpha/2); \quad r = (L_0 + l)\sin(\alpha/2); \quad R_0 = L_0\sin(\alpha/2). \tag{A36}$$

The local velocity profile at l is linear as in Eq (18), but with a dependence of the surface velocity v_l on l:

$$v_x(z; l) = v_l(l)z/h^S. \tag{A37}$$

This dependence can be found from the condition for constant total flow through any cross-section of the cone, $2\pi r h^S v_l/2 = const$, which yields:

$$v_l(l) = L_0 v_0/(L_0+l), \quad \text{and also} \quad v_L = \mathrm{d}L/\mathrm{d}t = L_0 v_0/(L_0+L). \tag{A38}$$

The membrane velocity is varying with the position l: it moves faster at the cone edge and slower with the increase of l. The flow of the liquid surface conserves its area, i.e., it does not create elastic strain in the membrane (we will skip the proof).

From now on, derivations are similar to the case of cylindrical flow in Section 3.1.1. The local dissipation rate per unit area [J/m^{2}s] is $w_{diss} = \eta^S v_l^2/h^S$, which must be integrated over the area of the cone, i.e., over $\mathrm{d}A_{cone} = 2\pi r\mathrm{d}l$:

$$W_{diss} = \int_{L_0}^{L} \frac{\eta^S v_l^2(l)}{h^S} 2\pi r\mathrm{d}l = 2\pi \sin\frac{\alpha}{2}\left(L + L_0\right)^2 \frac{\eta^S v_L^2}{h^S} \ln\frac{L + L_0}{L_0}; \tag{A39}$$

here we used Eqs (A38), and also the assumption that h^S and η^S are independent of l.

Next – the area of a cone is $\pi R_c(L + L_0)$, so the adhesion energy is:

$$F_{adh} = -A_{adh}\sigma_{adh} = -[\ \pi R_c(L+L_0) - \pi R_0 L_0\ ]\ \sigma_{adh}. \tag{A40}$$

Taking the time derivative of it, and using that $\mathrm{d}L/\mathrm{d}t = v_L$, we obtain for the power W_{adh} of the energy source the following expression:

$$W_{\mathrm{adh}} = \frac{\mathrm{d}F_{\mathrm{adh}}}{\mathrm{d}t} = -2\pi \sin(\alpha/2)(L+L_0)\sigma_{\mathrm{adh}} v_L = -2\pi R_{\mathrm{c}} v_L \sigma_{\mathrm{adh}} . \qquad \text{(A41)}$$

Eqs (A39) and (A41) are the conical analogues of the cylindrical Eqs (19) and (17). From the energetic balance ($W_{\mathrm{adh}} + W_{\mathrm{diss}} = 0$) one can find the velocity v_L of the patch edges:

$$v_L = \frac{\mathrm{d}L}{\mathrm{d}t} = \frac{h^{\mathrm{S}}\sigma_{\mathrm{adh}}}{\eta^{\mathrm{S}}(L+L_0)\ln(1+L/L_0)}; \qquad \text{(A42)}$$

compare to Eq (20). The integration of Eq (A42) yields:

$$t = \frac{\eta^{\mathrm{S}}}{2h^{\mathrm{S}}\sigma_{\mathrm{adh}}} L_0^2 \left[\left(1+\frac{L}{L_0}\right)^2 \ln\left(1+\frac{L}{L_0}\right) - \frac{L^2}{2L_0^2} - \frac{L}{L_0} \right]. \qquad \text{(A43)}$$

This is the conical variant of Lucas-Washburn Eq (21). For the sake of easier comparison, we can rewrite Eq (21) in a form similar to Eq (A43):

$$t = \frac{\eta^{\mathrm{S}}}{2h^{\mathrm{S}}\sigma_{\mathrm{adh}}} L^2 . \qquad \text{(A44)}$$

The dimensionless dependences of the cylindrical L on t and the conical L on t are given in Figure S 2 (the units of L and t are $[L_0]$ and $[\eta^{\mathrm{S}}L_0^2/2h^{\mathrm{S}}\sigma_{\mathrm{adh}}]$ respectively).

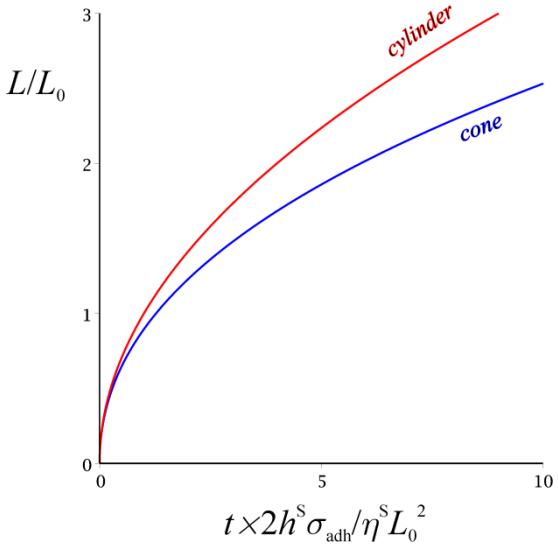

Figure S 2. Dimensionless wetted length vs. dimensionless time for cone and cylinder, Eqs. (A43)-(A44). This figure reflects the fact that at the point at which the patch starts to penetrate into the pipette, it sees only the radius R_0 which is the same for the cylinder and the cone. Wetted length L for the cone corresponds to more volume of liquid in the seal zone compared to a cylindrical pipette, which means higher friction and slower creep.

S6. Pressure-driven creep rate in conical capillary

The relevant Navier-Stokes equation in the lubrication approximation is:

$$\partial_l p(l) = \eta^{\mathrm{S}} \partial_{zz} v_x(z,l) .$$

Double integration with respect to z yields the velocity profile:

$$v_x(z,l) = \frac{z}{h^{\mathrm{S}}} v_l(l) + \frac{\partial_l p(l)}{2\eta^{\mathrm{S}}} z\left(z - h^{\mathrm{S}}\right). \tag{A45}$$

We need two conditions to determine the unknown functions $v_l(l)$ and $p(l)$. *The first condition* is for area conservation of the membrane (i.e., the membrane cannot stretch while flowing). A portion of the membrane of length δl is transferred for a period of time dt from point l to point $l + v_l \mathrm{d}t$. The membrane length is altered after this shift:

$$\delta l \to \left(1 + \partial_l v_l(l) \mathrm{d}t\right) \delta l ;$$

the respective area alteration is:

$$2\pi r(l)\delta l \to 2\pi r(l + v_l \mathrm{d}t)\left(1 + \partial_l v_l(l)\mathrm{d}t\right)\delta l \approx 2\pi r(l)\delta l + 2\pi \frac{\partial v_l(l) r(l)}{\partial l} \mathrm{d}t \delta l . \tag{A46}$$

From this equation it follows that if we assume that the membrane area is conserved, then $\partial_l(r v_l) = 0$ is fulfilled, which yields for v_l once again Eq (A38) (using Eqs (A36)). *The second condition* is the one for constant volume discharge through a cross-section of the cone, which is obtained by integration of Eq (A45):

$$Q = 2\pi r \int_0^{h^{\mathrm{S}}} v_x(z,l) \mathrm{d}z = const . \tag{A47}$$

The pressure drop between the two ends of the seal ($l = 0$ and $l = L$) is Δp, which allows us to find the unknown *const*. After some calculations, from Eq (A47) (a differential equation for the unknown function $p(l)$) and from the surface conservation condition, Eq (A38), we can obtain:

$$p(l) - p^{\mathrm{C}} = \left(p^{\mathrm{P}} - p^{\mathrm{C}}\right) \frac{\ln\left(1 + l/L_0\right)}{\ln\left(1 + L/L_0\right)} = \Delta p \frac{\ln\left(1 + l/L_0\right)}{\ln\left(1 + L/L_0\right)}, \tag{A48}$$

where p^{C} is the pressure in the cell outside the pipette; $p^{\mathrm{P}} = p^{\mathrm{C}} + \Delta p$ is the pressure in the pipette above the patch dome (outside the cell). Substituting Eq (A48) into Eq (A45), we obtain the velocity profile $v_x(z,l)$. From it the rate of dissipation of energy is calculated:

$$W_{\text{diss}} = \frac{2\pi\eta^{\text{S}}}{h^{\text{S}}} \sin\left(\frac{\alpha}{2}\right)\left(L_0 + L\right)^2 \ln\left(1 + \frac{L}{L_0}\right) v_L^2 . \tag{A49}$$

The mechanical work per unit time (if W_{flow} is neglected) is equal to $W_{\text{patch}} = \pi R_{\text{c}}^2 \Delta p v_L$, cf. Eq (25). From the balance $W_{\text{flow}} + W_{\text{patch}} = 0$, we find then the velocity at $l = L$:

$$v_L = \frac{\mathrm{d}L}{\mathrm{d}t} \approx -\frac{h^{\text{S}}}{2\eta^{\text{S}}} \frac{\Delta p}{\ln\left(1 + L / L_0\right)} \frac{R_{\text{c}}}{L_0 + L} . \tag{A50}$$

As with the cylinder (Section 3.1.2), some small terms, O(h/L), are neglected. This result is similar to Eq (A42) for adhesion-driven creep, with $-\Delta p R_{\text{c}}/2$ instead of σ_{adh}, as it was with cylindrical capillary. However, the pressure-driven creep of the patch will follow different dependence from the adhesion driven creep since R_{c} depends on L, cf. Eq (A36). Eq (A50) can be integrated:

$$t = \frac{2\eta^{\text{S}}}{h^{\text{S}} \Delta p \sin(\alpha / 2)} \left[\left(L + L_0\right) \ln\left(1 + L / L_0\right) - L\right]. \tag{A51}$$

If adhesion force and pressure gradient are acting simultaneously, the energy balance is $W_{\text{flow}} + W_{\text{patch}} + W_{\text{adh}} = 0$, cf. Eqs (A49), (A41) and (25). It yields:

$$v_L = \frac{\mathrm{d}L}{\mathrm{d}t} \approx -\frac{h^{\text{S}}}{\eta^{\text{S}}} \frac{\Delta p R_{\text{c}} / 2 - \sigma_{\text{adh}}}{\left(L_0 + L\right) \ln\left(1 + L / L_0\right)} . \tag{A52}$$

S7. Experimental data for pressure-driven creep

Protein incorporation into liposomes.

D/R method. This method followed closely that described by Häse et al.[48] (1). Lipids (2 mg) were dissolved in a glass test tube using chloroform. D/R buffer (1 mL) was added, and the solution sonicated for 15 min to form a cloudy liposome suspension. This was transferred into a 15 mL falcon tube, and a further 2 mL of D/R buffer was added. The desired quantity of MscS and/or MscL was then added at a protein to lipid ratio of 1:1000 (wt/wt) for both proteins and the solution was placed on a rotary wheel for 1 h at 4°C. After this time, Bio-Beads SM-2 (BioRad, Richmond, CA) were added and the suspension mixed for a further 3 h. The solution was centrifuged at 250 000 × *g*, and the pellet was collected and spotted onto a microscope cover glass, and dehydrated under vacuum overnight at 4°C. The dried lipid spot was rehydrated with D/R buffer at 4°C and subsequently used for experimentation.

Sucrose method. A total of 2 mg of a lipid or a mixture of lipids dissolved in chloroform was dried under a stream of N_2 gas. Distilled water (5 μL) was then added to prehydrate the lipids, followed 5 min later by 1 mL of 0.4 M sucrose. The solution was placed in the oven at 55 °C for 3 h, after which time, the appropriate volume of MscS and MscL was added to make a protein-to-lipid ratio of 1:1000 (wt/wt) for both proteins.

Electrophysiology.

Before gigaohm-seal formation and excision of membrane patches from liposome blisters, an aliquot of liposomes (2-4 μL) was placed on the bottom of the experimental chamber containing the bath solution. Liposome blisters were patched ~10 min after seeding of the liposome preparation. Negative pressure (suction) was applied to patch pipettes using a syringe and was monitored using a piezoelectric pressure transducer (PM 015R, World Precision Instruments, Sarasota, FL). Borosilicate glass pipettes (Drummond Scientific Co., Broomall, PA) were pulled using a pipette puller (PP-83, Narishige, Tokyo, Japan). Electrodes with resistance of 2.5–5.0MΩ (bubble number, 4.0–5.0) were used for the patch-clamp recording from inside-out liposome patches. To confirm whether MscS and/or both MscS and MscL were included in the liposomal membranes, the channel activities of both channels were examined in liposomes using the patch-clamp method. Currents were amplified with an AxoPatch 1D amplifier (Axon Instruments),and

data were acquired at a sampling rate of 5 kHz with 2kHz filtration. The bath and pipette recording solution were the same consisting of 200 mM KCl, 40 mM $MgCl_2$, and 5 mM HEPES (pH 7.2 adjusted with KOH).

Fluorescence imaging of membrane patches.

Fluorescence images from excised inside-out membrane patches, which consisted of azolectin (99.9 weight %)/rhodamine-PE (0.1%) containing wild-type MscS and/or both MscS and MscL and azolectin (69.9%)/cholesterol (30%)/rhodamine-PE (0.1%) membranes were observed using a confocal microscope (LSM 700, Carl Zeiss Inc., Jena, Germany) specially placed in a patch-clamp Faraday cage using a long working distance water immersion objective lens (63x, NA1.15, Carl Zeiss, Jena, Germany). A 555 nm laser was used as the excitation light source. Fluorescence data were acquired and analyzed with ZEN software (Carl Zeiss Inc., Jena, Germany). Scan rate was 196 ms/scan, with no interval between consecutive scans. To visualize liposome patches the pipette tip was bent ~30° with a microforge (Narishige; MF-900, Tokyo, Japan) to become parallel to bottom face of the chamber.

A typical measurement is illustrated in Figure S 3 with data for MscS+MscL. After the patch is formed, pressure is applied and this pressure is increased stepwise, approximately linearly with time (Figure S 3, up). Simultaneously, creeping distance $\Delta L = L(t) - L(0)$ was monitored as function of time (Figure S 3, down). The ΔL data was used to calculate the creeping velocity v_L according to Eq (60). Together with the pressure data, this allows the construction of the plot in Figure 6.

Dome bulging results in deviation of the creep velocity from Eq (61), cf. Figure 6. The observed geometry of the patch during creep under the action of suction is shown in Figure S 4. Only after the dome has relaxed to a stationary shape is Eq (61) valid.

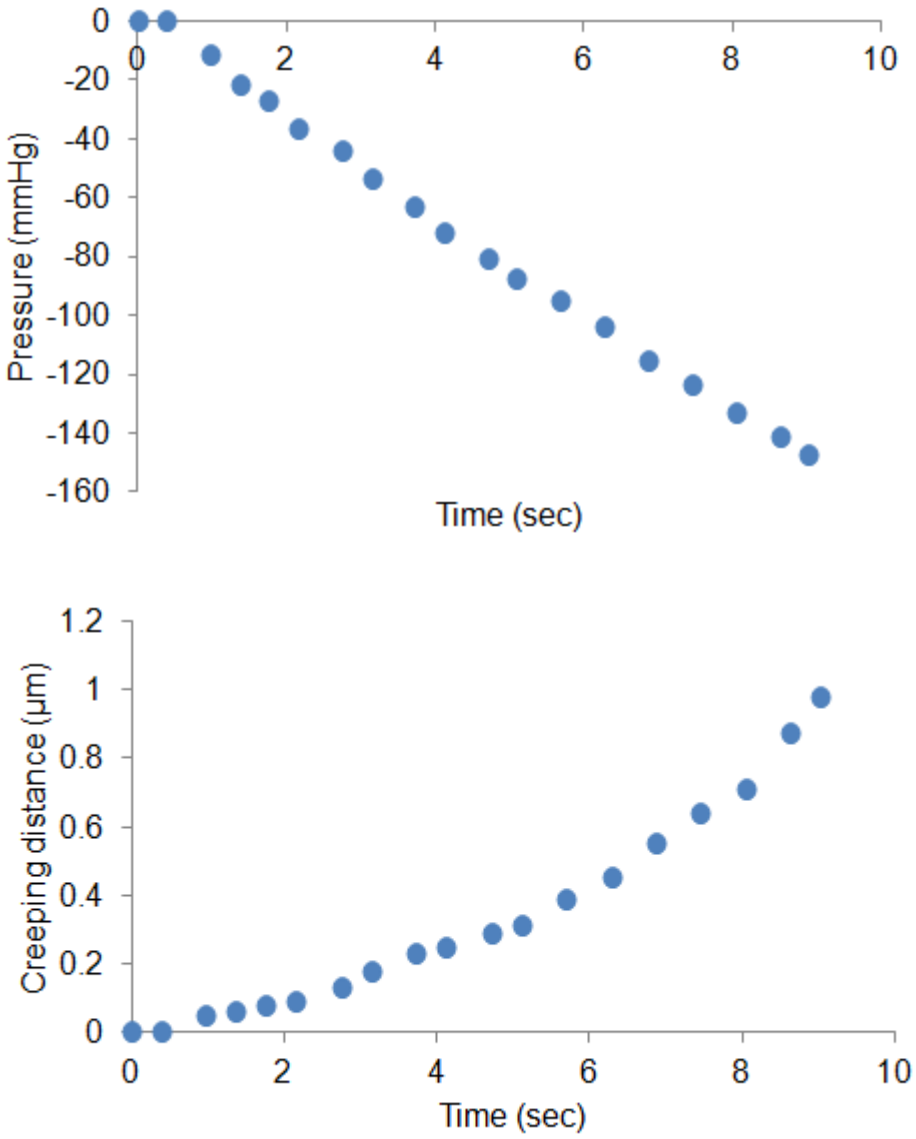

Figure S 3. Applied pressure vs. time and creeping distance $\Delta L = L(t) - L(0)$ vs. time. Data for MscS+MscL.

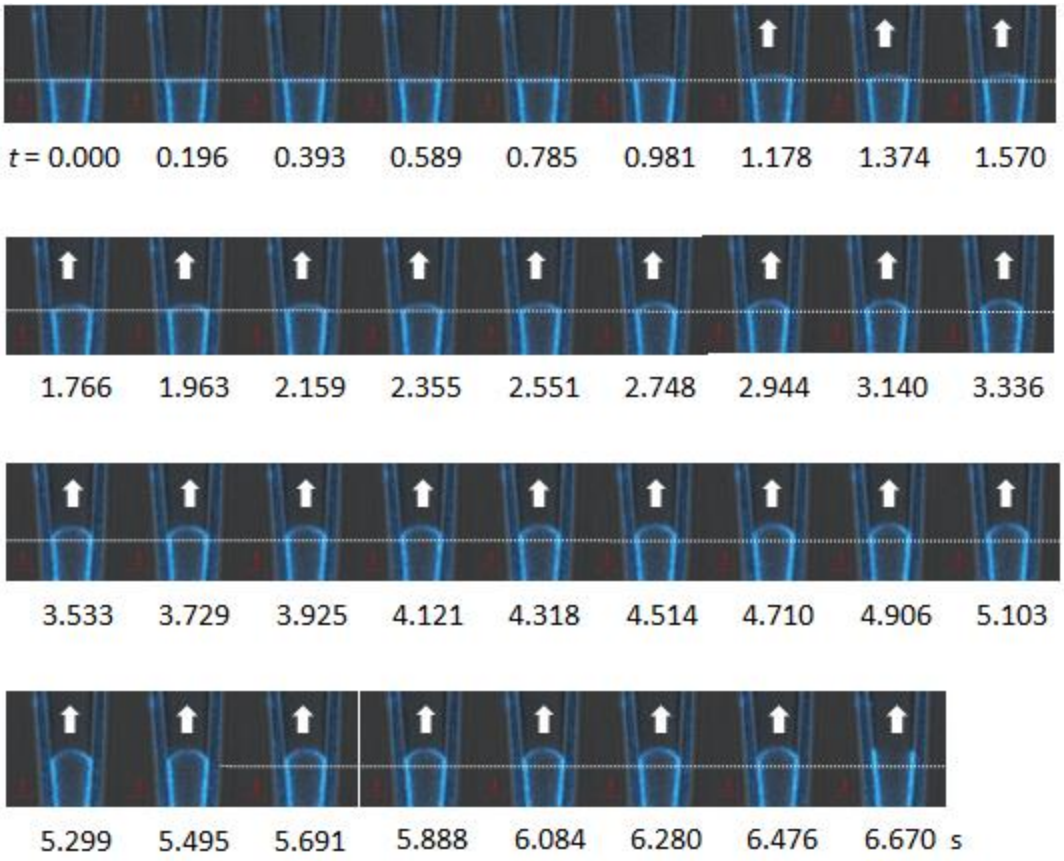

Figure S 4. Series of confocal single frame images (MscS patch) illustrating the typical patch behavior under the action of increasing pressure. The pressure starts to increase linearly at 1.18 s. Initially, the patch dome bulges until at t = 5 s it relaxes to a stationary shape. At this stage, the patch continues to creep according to Eq (A50), until the lytic pressure Δp = 7800 Pa is reached at t = 6.670 s.